THE JOURNAL OF PHYSICAL CHEMISTRY C

Article

pubs.acs.org/JPCC

Ionization Probability in Molecular Secondary Ion Mass Spectrometry: Protonation Efficiency of Sputtered Guanine Molecules Studied by Laser Postionization

Nicholas J. Popczun,[†] Lars Breuer,[†] Andreas Wucher,[*,‡] and Nicholas Winograd[†]

[†]Department of Chemistry, The Pennsylvania State University, 104 Chemistry Building, University Park, Pennsylvania 16802, United States

[‡]Fakultät für Physik, Universität Duisburg-Essen, 47048 Duisburg, Germany

Supporting Information

ABSTRACT: The prospect of improved secondary ion yields for secondary ion mass spectrometry (SIMS) experiments drives innovation of new primary ion sources, instrumentation, and postionization techniques. An important factor affecting the detection sensitivity in molecular SIMS and other desorption techniques as well is believed to be the poor ionization probability of a sputtered molecule, a value which is often assumed to be as low as 10^{-5} but at present is basically unknown. In order to estimate how much headroom there is for future developments toward strategies aimed at enhancing the ionization probability, we study the protonation efficiency of sputtered guanine molecules for formation of $[M + H]^+$ secondary ions using strong field laser postionization (LPI) to detect the corresponding neutral molecules. In order to allow a quantitative comparison of secondary ion and neutral yields, the postionization signal is corrected for undersampling of the principally detectable plume of sputtered neutral particles by the focused laser beam. It is shown that the protonation probability of molecular guanine desorbed from a clean film under bombardment with 20 keV C_{60} cluster projectiles is of the order of $1-2 \times 10^{-3}$, with some remaining uncertainty arising from laser-induced fragmentation and possible differences in the emission velocity distributions of neutral and ionized molecules. Moreover, we find that the postionization signal can in principle be boosted by 2 orders of magnitude if a more powerful ionization laser is employed.

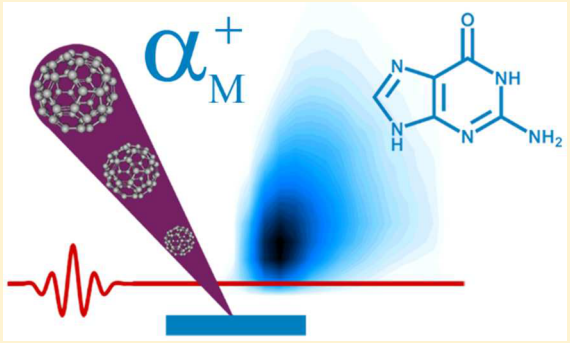

1. INTRODUCTION

Secondary ion mass spectrometry (SIMS) is a powerful tool for chemical imaging due to the submicron spatial resolution and the ability to obtain molecular information during an experiment.[1,2] Molecular imaging of organic compounds has benefitted from increased sensitivity provided by the introduction of new primary ion projectiles such as metal, fullerene, or gas clusters. Typically, these projectiles increase the sputter yield and reduce the collision-induced damage remaining in the sample surface, although the useful ion yield obtained particularly for molecular systems is generally still low. This situation is often attributed to a poor ionization efficiency of the sputtered molecules, thereby triggering the development of strategies to design chemically active cluster projectiles in order to enhance the ionization efficiency. For instance, it has been demonstrated that water cluster projectiles can in some cases significantly enhance useful molecular secondary ion yields at comparable total sputter yield with respect to rare gas cluster ion beams.[3,4] Using a different approach, our group has developed a strategy to dope reactive species into a rare gas cluster projectile in order to boost the chemical ionization efficiency.[5,6] In all cases, however, the measured useful yield, i.e., the number of detected molecular secondary ions divided by the total number of sputtered molecule equivalents, is still rather low,[6] an observation that suggests poor ionization efficiency limits the measured values.

Many factors influence the value of the useful molecular ion yield. These factors include the ability of a molecule to survive the violent sputtering process without fragmentation, the probability of ionization during emission (including a possible reneutralization of a molecular secondary ion), and the instrumental collection and detection efficiency for the resulting secondary ion. To guide strategies for further improvement, it is helpful to investigate the role of each of these different contributing factors separately. Here, we focus on the determination of the ionization probability of a sputtered intact parent molecule in order to estimate how much headroom there is for future enhancements of molecular useful ion yields by strategies aimed at enhancing this quantity. In fact, such improvements are urgently needed particularly in imaging

Received: February 14, 2017
Revised: March 29, 2017
Published: March 30, 2017

DOI: 10.1021/acs.jpcc.7b01467
J. Phys. Chem. C 2017, 121, 8931−8937

experiments since as pixel and voxel sizes of two- and three-dimensional chemical images decrease the number of molecules contained within a voxel grows fewer, so conversion of these molecules to detected molecular ions is crucial for generating chemically informative images.

A quantitative determination of ionization probabilities in sputtering requires the simultaneous detection of secondary ions and their neutral counterparts under otherwise identical experimental conditions. Time-of-flight SIMS instruments equipped with laser postionization have been demonstrated to be well suited for such a task.[7,8] Using this methodology, quantitative estimates of absolute ionization probability values have been reported for inorganic metal or semiconductor atoms and clusters sputtered from the respective clean surfaces.[9−20] Recently, this method has also been applied to the study of organic molecules.[21,22] One of the fundamental problems here is that the postionization laser needs to be capable of efficient photoionization of a sputtered molecule without excessive photofragmentation. Basically, two strategies have proved successful in this respect. Single photon ionization, on one hand, may constitute a "soft" ionization mechanism[8,23] but requires the photon energy to be above the ionization energy of the targeted molecule, a requirement which for most organic molecules is hard to fulfill with sufficiently high photon flux to allow efficient postionization.

The strategy pursued in our lab, on the other hand, utilizes strong field photoionization in the near-infrared wavelength range,[8] which was shown to permit the intact ionization of many organic molecules.[24,25] Since this technique requires relatively high laser power densities in order to be efficient, it can at present only be used in connection with tightly focused laser beams which sample only a small portion of the detectable plume of sputtered neutral particles. We have recently developed a method to correct for this undersampling effect by scanning the laser beam across the sensitive volume above the bombarded surface, i.e., the volume capable of ion extraction and detection in the mass spectrometer.[21,22,26] The resulting integrated postionization signal can then be directly compared with the respective secondary ion signal extracted from the same volume in order to deliver a quantitative estimate of the ionization probability. Respective data obtained for coronene molecules sputtered from a coronene film held at room temperature have delivered a probability for the formation of M^+ molecular ions of the order of 10^{-3}.[22] In the present work, we apply the method to guanine as a biologically relevant molecule. Moreover, the sample is held at low temperature throughout the analysis in order to reduce the background arising from evaporated gas-phase molecules. The results reveal a much more detailed representation of the detectable plume of sputtered neutral molecules, which is shown to deviate considerably from that measured for gas-phase molecules. The ionization probability of the intact guanine molecules sputtered by 20 keV C_{60}^+ primary ions is estimated to be of the order of $1-2 \times 10^{-3}$.

2. EXPERIMENTAL SECTION

The time-of-flight (ToF) SIMS instrument used in these experiments has been described elsewhere.[27] In brief, the instrument employs a 40 keV C_{60}^+ primary ion gun (Ionoptika IOG C60−40, Ionoptika Ltd., Southampton, UK),[28] a temperature-controlled sample stage, and a calcium fluoride (CaF_2) window to allow integration of radiation for laser ionization. Depth profiles were obtained by alternating a 20 keV C_{60}^+ primary ion beam of 85 pA current between 5 s dc etch cycles at a field of view (FOV) of 250 × 250 μm^2 and analytical cycles consisting of 10 000 primary ion pulses rastered over a FOV of 100 × 100 μm^2. A primary ion pulse length of 2000 ns was used, which was shown to be long enough to ensure a stationary distribution of sputtered particles in the probed volume above the surface (see Figure S1 in the Supporting Information).[29] As described in detail elsewhere,[8] the signal measured under these conditions represents the number density of the emitted particles which is integrated over their entire velocity distribution. In order to restrict the sensitive volume of the time-of-flight mass spectrometer in the direction toward the sample surface, the reflectron voltage was set at 98% of the sample potential generating the ion extraction field, ensuring that ions originating from distances less than about 0.5 mm above the bombarded surface are excluded from detection. In addition, the time refocusing and ion optical properties restrict the sensitive volume in the directions toward the extraction optics and parallel to the surface, respectively, thereby allowing us to observe postionized neutrals and secondary ions under otherwise identical experimental conditions as described in more detail previously.[7,8,29]

Laser ionization of thermally evaporated and sputtered molecules was performed with a commercially available chirped pulse amplification laser system (Coherent Legend Elite Duo, Santa Clara, CA, USA) and optical parametric amplifier (OPA) (Light Conversion TOPAS-C-HE, Vilnius, Lithuania), providing 1500 nm, 40 fs radiation, focused with a 150 mm (at 587.6 nm) BK-7 lens positioned outside the analysis chamber to a peak power of 4×10^{14} W/cm^2. At the beginning of each experiment, the position of the laser beam was optimized for maximum LPI signal. Guanine films were deposited on 10 × 10 mm Si shards (Ted Pella Inc.) to thicknesses of ∼220 nm, measured by a quartz crystal microbalance (QCM). With the exception of the thermal desorption measurements, all experiments were performed with the sample kept at low temperature (∼100 K) in order to reduce the signal background originating from gas-phase molecules.

3. RESULTS AND DISCUSSION

The goal of this work is to determine the SIMS ionization probability for sputtered guanine molecules by quantitatively comparing the $[M + H]^+$ secondary ion signal and the M^+ photoion signal arising from laser postionization of neutral molecules M present in the sensitive volume of the TOF mass spectrometer. The method has been explained in great detail elsewhere.[22] In brief, the effect of a collision-induced chemical modification of the surface ("damage") on the ionization probability, the loss of neutral molecular signal from photofragmentation, as well as the relationship between the effective photoionization volume and the extension of the sensitive volume must be characterized. For the latter, it has been shown that the focused laser employed in these experiments significantly undersamples the entire plume of principally detectable neutral molecules and must therefore be scanned across the plume with the signal being summed over the scan.[22,26] The SIMS ionization probability can then be calculated according to

$$\alpha_M^+ = \frac{S^+}{S^+ + \frac{1}{\varphi\upsilon}\sum_{i,j} S_{i,j}^0 + S^-} \quad (1)$$

DOI: 10.1021/acs.jpcc.7b01467
J. Phys. Chem. C 2017, 121, 8931−8937

where α_M^+ is the positive ionization probability; S^+ is the measured secondary positive ion signal; $S_{i,j}^0$ is the signal of postionized neutral molecules measured with the laser positioned at the scan position (i,j); S^- is the measured secondary negative ion signal; υ is a correction factor determined by the volumetric overlap of the effective photoionization volume sampled by the laser and the voxel size of the laser raster scan steps; and φ is the fraction of molecules that survive the photoionization process intact.

3.1. Fluence Dependence. The individual molecular SIMS and LPI signals are shown as a function of the primary ion fluence in Figure 1a. Both signals experience an exponential decay before reaching steady state at a fluence of about 2.5×10^{13} ions/cm^2, henceforth referred to as the critical dose. The initial decay is due to accumulation of chemical damage and can be characterized using the erosion dynamics model.[30,31] The ratio of the steady state LPI signal to that measured at the surface before bombardment is 0.31, while the same ratio for the SIMS signal is 0.36. It can also be seen that the LPI signal determines the critical dose, with the SIMS signal apparently reaching a steady state slightly before that of the postionized neutral molecules. These discrepancies demonstrate the action of the bombardment-induced chemical damage toward modifying the protonation probability of sputtered molecules.

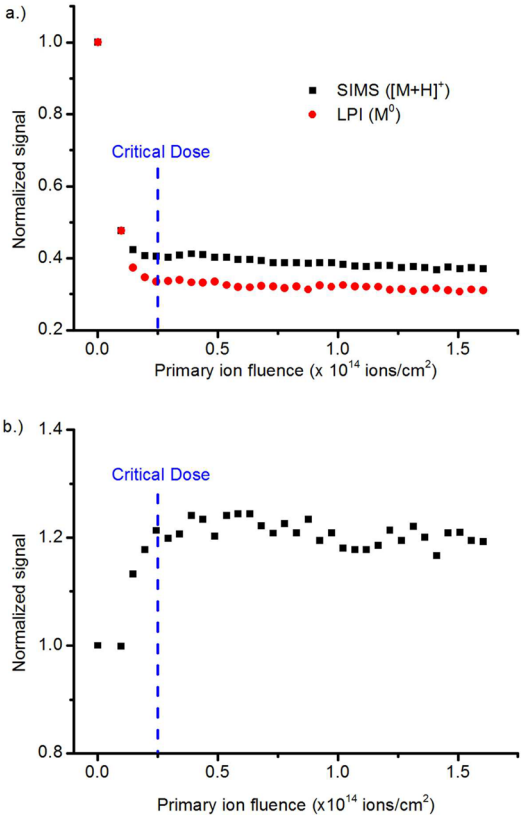

Figure 1. Molecular SIMS ($[M + H]^+$ at m/z 152) and LPI ($[M]^+$ at m/z 151) signals (a) and ratio between both signals (b) of guanine molecules sputtered under bombardment with 20 keV C_{60}^+ ions as a function of primary ion fluence. The data were normalized to the value obtained for a pristine surface at zero fluence.

The relative variation of the ionization probability under prolonged ion bombardment can be found from the ratio between both signals shown in Figure 1a. The result is depicted in Figure 1b. The initial data point depicted at zero fluence was obtained under static conditions, i.e., with a fluence of about 10^{11} ions/cm^2 used to take a spectrum, which ensures that each primary ion impinges onto a previously unaltered part of the sample surface. The remaining data points were then normalized to this static value. The figure shows that the protonation probability of sputtered guanine molecules increases by about 20% with increasing primary ion fluence and reaches a steady state at the critical dose. This finding indicates an accumulative effect where the chemical modification of the surface produced by previous impacts apparently enhances the protonation efficiency, for instance by liberation of free protons.[32]

The establishment of steady state conditions as shown in Figure 1 is in agreement with earlier studies performed on the same system.[33] It is essential because a laser beam scan across the entire detectable plume of sputtered neutral molecules, as is needed to estimate the absolute value of the ionization probability, requires acquisition of several hundred individual mass spectra to be recorded in succession. Steady state conditions ensure that the measured signal does not fluctuate during the acquisition of such a scan, for instance by a primary ion fluence-dependent sputter rate.

3.2. Photofragmentation. A mass spectrum of photoions obtained from thermally evaporated guanine molecules is shown in Figure 2a. In this case, it is fair to assume that the precursor prior to photoionization is just the intact neutral molecule with negligible thermal internal energy. For reasons explained below, the spectrum is only shown for the mass-to-

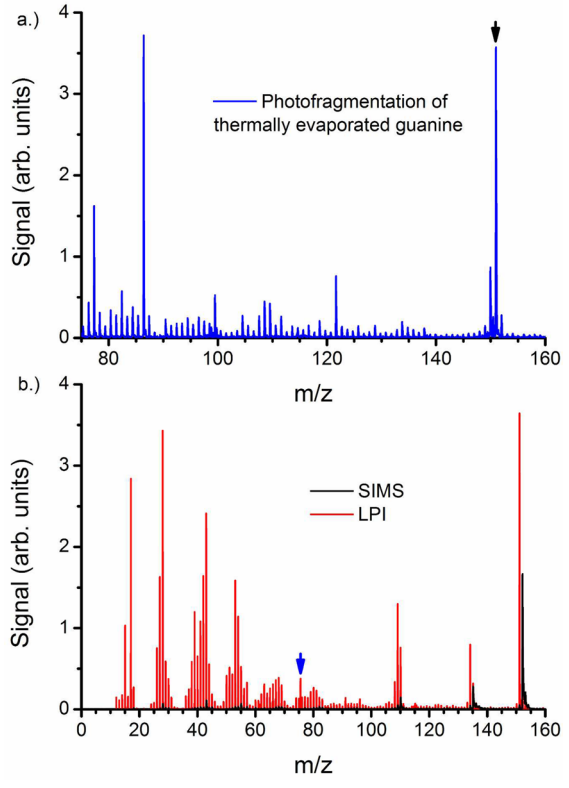

Figure 2. Mass spectrum of thermally evaporated (a) and sputtered (b) guanine for the determination of upper and lower limits for the photofragmentation branching ratio. The arrows indicate the molecular ion signal at m/z 151 ($[M]^+$) and m/z 152 ($[M + H]^+$), respectively. The arrow at m/z 75.5 in (b) refers to the doubly charged molecular ion.

DOI: 10.1021/acs.jpcc.7b01467
J. Phys. Chem. C 2017, 121, 8931−8937

charge range greater than m/z 75.5. It is seen that in this range the spectrum is dominated by the molecular $C_5H_5N_5O^+$ ion at m/z 151 along with a $C_2H_5N_3O^+$ fragment at m/z 87, with proposed structures shown in Figure 3a and 3b, respectively.

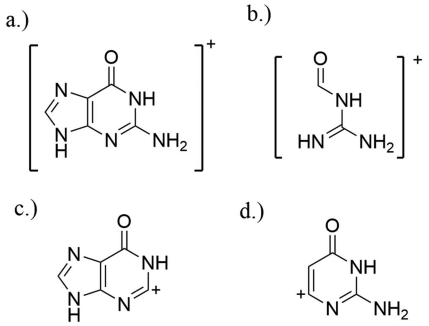

Figure 3. Proposed structures for the molecular photoion (a), photofragment at m/z 87 (b), and collision-induced fragments m/z 135 (c) and m/z 110 (d).

This fragment is formed by a cleavage between the two rings of the guanine molecule followed by addition of two hydrogen atoms to saturate the dangling bonds. In order to estimate the total photofragmentation probability of an intact guanine molecule according to

$$M + h\nu \rightarrow F_1^+ + F_2 \tag{2}$$

we make the crude assumption that all fragments F_i are photoionized and contribute to the measured spectrum with comparable efficiency. Since the sum of the fragment masses must equal the mass of the original parent molecule, it is sufficient to scan the spectrum in the m/z range between the half and full molecular mass. This procedure ensures that each detected photofragment must originate from a distinct, thermally evaporated parent molecule and that each fragmentation reaction 2 is therefore counted only once. Comparison of the molecular ion signal to the integrated total ion signal depicted in Figure 2a therefore allows us to estimate a photofragmentation probability of about 85%, indicating that about 15% of the thermally evaporated guanine molecules survive the photoionization process intact. Since the sputtered molecules may contain substantial amounts of internal energy and are therefore probably more prone to photofragmentation, this value constitutes a lower limit of the photofragmentation probability that will occur during an LPI experiment.

We wish to note that the spectrum measured for evaporated material also includes a signal at m/z 302, corresponding to guanine dimers. It is interesting to note that this signal also appears in the SIMS spectrum taken at the pristine sample surface, indicating that dimers are also being generated in the more energetic sputtering process. In both cases, however, the signal is small compared to the monomer signal, so that we neglect dimer formation in the determination of the fragmentation probability.

In addition to the SIMS spectrum, Figure 2b shows an LPI spectrum obtained at the pristine sample surface. Note that this spectrum was measured with the low mass ion suppression normally employed to avoid detector saturation being switched off. Moreover, the background signal arising from photoionization of the residual gas was eliminated by subtracting the spectrum taken without the ion bombardment. To determine an upper limit for the photofragmentation that will occur during an LPI experiment, the molecular guanine signal observed in Figure 2b is compared to the sum of the total ion signal. This treatment assumes that only molecular guanine is sputtered from the sample surface and that all signals observed at other mass-to-charge ratios are strictly due to photofragmentation, with each fragment arising from an unfragmented parent molecule. This way, an upper limit of 92% is estimated for the photofragmentation probability, leaving about 8% of the sputtered molecules intact. As explained above, however, these assumptions are likely to lead to a significant overestimation of the fragmentation probability since (i) low mass fragments arising from the same fragmentation chain reaction may contribute multiple times and (ii) the signal contribution arising from photoionization of collision-induced neutral fragments produced in the sputter ejection process is neglected. From the SIMS spectrum, on the other hand, it is evident that there are collision-induced fragments at m/z 135 and m/z 110, shown in Figure 3c and 3d, respectively, as well as some smaller fragments at mass-to-charge ratios less than m/z 60.

The bracketing values for the photofragmentation probability of a sputtered intact guanine molecule determined above introduce a primary source of uncertainty of the order of a factor of two in the ionization probability as calculated using eq 1. Nevertheless, the data indicate that the branching ratio φ, i.e., the probability for a sputtered guanine molecule to survive the postionization process intact, amounts to approximately 10%.

3.3. Undersampling Correction. As noted above, the spatially focused laser beam required for strong-field photoionization does not overlap the entirety of principally detectable sputtered neutral material in a single experiment. Therefore, the undersampling of the principally detectable plume of sputtered neutral molecules is characterized by scanning the laser beam horizontally and vertically with respect to the sample surface and repeating the experiment at different positions of the focal volume, thereby integrating the measured postionization signal. The integration process requires knowledge of the effective ionization volume sampled by the laser in a single experiment, which is estimated by determining the laser intensity I_{sat} required to saturate the photoionization process. As described in detail elsewhere,[21,24,34] the value of I_{sat} is identified by plotting the photoion signal for the selected neutral component as a function of the natural log of the peak intensity, I_0, in the center of the laser beam. When $I_0 \gg I_{sat}$, this plot asymptotically follows a straight line describing the ionization volume expansion with increasing laser intensity, which can be extrapolated to the $\ln(I_0)$ axis to determine I_{sat}. For the molecular guanine LPI signal, this is illustrated in Figure 4, yielding $I_{sat} = 7 \times 10^{13}$ W/cm^2. The effective ionization volume is then defined by all points in space with laser intensity $I \geq I_{sat}$, delivering an effective ionization radius R' described by[34]

$$R' = R\sqrt{\ln(I_0/I_{sat})} \tag{3}$$

where R is the distance from the beam center where the laser intensity has fallen to I_0/e and $\pi R'^2$ denotes the cross section of the effective ionization volume in the direction perpendicular to the beam propagation.

Using $R = 27$ μm, calculated from the parameters of the unfocused beam, the effective radius at our setting of $I_0 = 4 \times 10^{14}$ W/cm^2 is calculated as $R' = 35.5$ μm. In order to determine the integrated postionization signal, the signal measured at each laser position is summed, and a correction

DOI: 10.1021/acs.jpcc.7b01467
J. Phys. Chem. C 2017, 121, 8931−8937

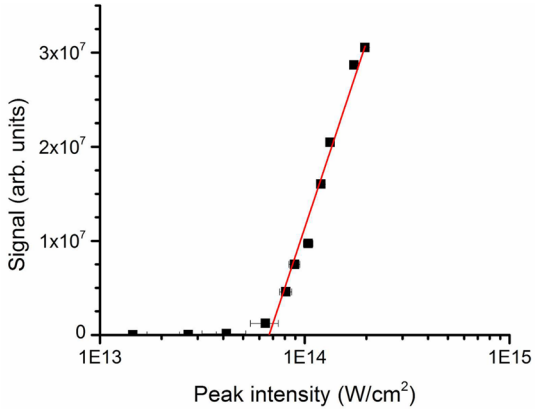

Figure 4. Signal of laser postionized guanine molecules $[M]^+$ vs natural log of the peak laser intensity. The asymptote intersects the laser intensity axis at the saturation intensity of about 7×10^{13} W/cm^2.

factor $\upsilon = \pi R'^2/\Delta x \Delta y$ is applied to account for the difference between the volume effectively sampled by the laser and the voxel size given by the translation steps of Δx and Δy during the laser beam scan. For the experiments performed here, the factor was found to be $\upsilon = 0.40$.

3.4. Measured Neutral Molecular Guanine Signal. As described above, the laser was scanned through the plume of principally detectable sputtered neutral molecules to create the two-dimensional image shown in Figure 5. The signal at each

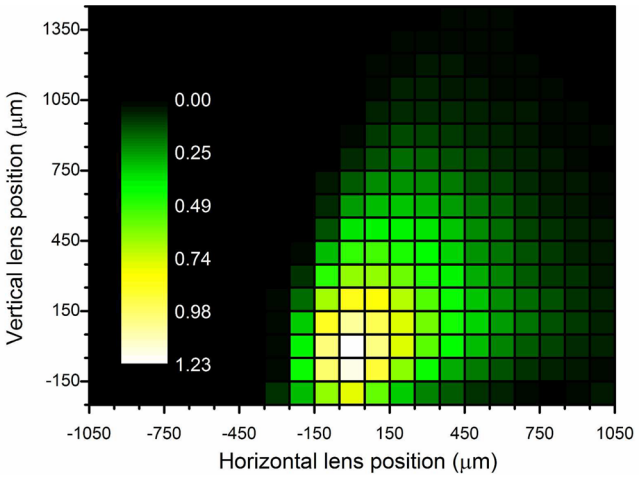

Figure 5. Measured signal of postionized sputtered neutral guanine molecules vs lateral position of the ionizing laser beam. The laser was scanned in the plane perpendicular to the beam propagation along vertical and horizontal directions with respect to the sample surface. The axes are scaled with respect to the position for optimum detected signal, and the intensity scale has been normalized to the measured SIMS signal.

position was normalized to the SIMS signal, which was recorded with the postionization laser beam blocked. The resulting total signal of postionized neutral guanine molecules summed from all 357 laser positions was 109 times the SIMS signal. Comparing the total integrated signal with the signal measured with the laser beam adjusted to the position delivering optimal LPI signal, one finds that under optimized conditions a single LPI experiment only samples about 1.1% of the entire detectable plume.

In previous applications of this technique to estimate the ionization probability of sputtered β-estradiol[21] and coronene[22] molecules, the laser beam was vertically scanned only upward from the optimal laser position since the beam could not be moved closer to the sample without starting to ablate surface material. In the present work, the sensitive volume was moved farther away from the surface by slightly lowering the reflection voltage. Moreover, the experiment was performed with the sample held at low temperature, so that the density of gas-phase molecules evaporated from the surface was greatly reduced. As a consequence, the entire detectable plume could be mapped without ablation of the sample surface, and particularly the signal originating from sputtered molecules at laser positions located beneath the optimal position could be clearly identified.

A laser scan with no primary ion bombardment was performed in order to map the sensitive volume for gas-phase species as well. As an example, a plot of the signal recorded at m/z 78 under these conditions is presented in Figure 6. It is

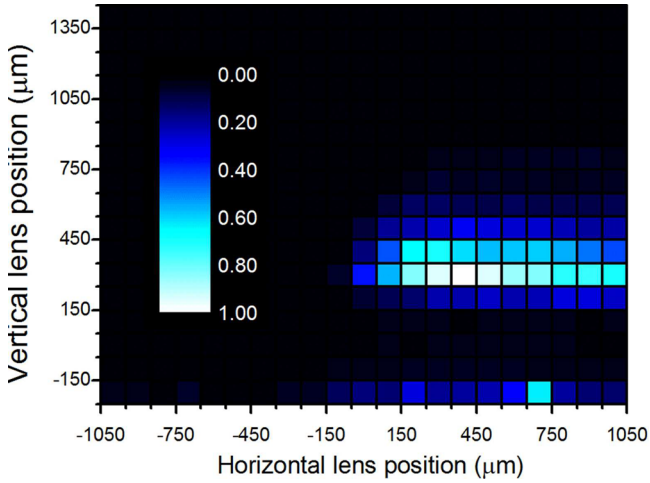

Figure 6. Measured signal of photoionized gas-phase benzene molecules vs position of the ionizing laser beam. The laser was scanned in the plane perpendicular to the beam propagation along vertical and horizontal directions with respect to the sample surface and the extraction volume. The axes are scaled the same as in Figure 5.

noteworthy that the sensitive volume for gas-phase species is different from that for sputtered species. More specifically, we find maximum gas-phase signal to originate from a laser position which is shifted by about 300 μm above and 300 μm in the direction of the primary ion flight path from that delivering maximum sputtered guanine signal. As explained in more detail in the Supporting Information, we attribute this finding, which has been reported before,[21] to the emission velocity and angle distribution of the sputtered molecules along with the ion optical settings of the mass spectrometer.

3.5. Ionization Probability. With the photofragmentation and undersampling characterized, the ion/neutral ratio within the sensitive volume of the mass spectrometer can be determined according to eq 1. Since the SIMS signal measured for negative molecular ions is small, it is neglected in the following. Depending on whether the minimum or maximum estimate of the photofragmentation probability is used, this results in ion/neutral ratio values between 7.6×10^{-4} and 1.5×10^{-3} under steady state sputtering conditions. To interpret these values in terms of the ionization probability, it is important to realize that the experiment performed here is

DOI: 10.1021/acs.jpcc.7b01467
J. Phys. Chem. C 2017, 121, 8931−8937

sensitive to the number density of sputtered particles rather than their flux. The ionization probability, on the other hand, refers to the partial sputter yields of secondary ions and neutrals and, hence, reflects a flux ratio. If the emission velocity distributions of sputtered ions and neutral species were significantly different, the conversion from measured density to flux would introduce a correction to the measured value of the ionization probability. A detailed discussion of the conversion along with an estimate of its possible influence is presented in the Supporting Information (Figure S3 and surrounding text), indicating that the number density ratio measured here may in principle lead to an underestimation of the ionization probability, with the magnitude of the effect being of the order of a factor of two. Therefore, the uncertainty introduced by the velocity effect appears to be of similar magnitude as that introduced by the photofragmentation issue and therefore does not change the order of magnitude of the measured value. As a consequence, we conclude that the ionization probability, i.e., the probability for a sputtered intact guanine molecule to form a protonated $[M + H]^+$ secondary ion, is about $1-2 \times 10^{-3}$.

The protonation probability determined here for guanine agrees well with the estimate of the ionization probability of coronene molecules sputtered from a fresh coronene film determined under similar bombardment conditions.[22] Note that the coronene experiment was performed at room temperature, which led to a significantly higher background signal originating from laser ionization of thermally desorbed molecules. Therefore, the high density of these species close to the surface did not allow the measurement of photoionized sputtered neutral molecules at laser positions located below the optimal position. In addition, the uncertainty introduced by the photofragmentation issue is improved nearly 5-fold with respect to that of the coronene experiment, providing a much smaller bracketing range for the determined ionization probability value.

4. CONCLUSION

From the quantitative comparison of the molecular secondary ion signal with that obtained by postionization of the corresponding neutral precursor molecules, we arrive at a measured value of about $1-2 \times 10^{-3}$ for the protonation probability of sputtered guanine molecules under bombardment with 20 keV C_{60}^+ ions. This value agrees well with the order of magnitude estimate published earlier for coronene molecules sputtered under similar bombardment conditions. It is of great interest since it allows us to judge the degree of opportunity to improve the detection sensitivity of molecular SIMS experiments via an enhancement of the ionization efficiency. In that sense, what is important is the correct order of magnitude rather than the exact value of the ionization probability, so that the still existing ambiguity with respect to the influence of photofragmentation on one hand and possible emission velocity effects on the other hand is probably of minor importance.

The data presented here indicate that there is headroom for improving the ionization efficiency of a sputtered intact molecule by 2 to 3 orders of magnitude as compared to 20 keV C_{60}^+ bombardment. This information is important in order to guide new strategies to improve the sensitivity particularly in SIMS imaging experiments, for instance by designing new optimized, chemically active projectile ions. On the other hand, quantitation of the degree of undersampling in the laser postionization experiment indicates that the molecular postionization signal, which is at present comparable to the molecular SIMS signal, can in principle be boosted by 2 orders of magnitude provided a more intense ionization laser would be available, which could then be defocused to sample the entire detectable plume of sputtered neutral molecules while still maintaining saturation ionization conditions.

■ ASSOCIATED CONTENT

Supporting Information

The Supporting Information is available free of charge on the ACS Publications website at DOI: 10.1021/acs.jpcc.7b01467.

Material to further explain the effective sensitive volume of the mass spectrometer, the influence of the primary ion pulse width, and the difference between ion and neutral emission velocity distributions (PDF)

■ AUTHOR INFORMATION

Corresponding Author

*E-mail: andreas.wucher@uni-due.de.

ORCID

Nicholas J. Popczun: 0000-0002-2631-8581

Author Contributions

The manuscript was written through contributions of all authors. All authors have given approval to the final version of the manuscript.

Notes

The authors declare no competing financial interest.

■ ACKNOWLEDGMENTS

The authors acknowledge the Department of Energy under grant DE-FG02-06ER15803 for their financial support of this research.

■ REFERENCES

(1) Winograd, N. The Magic of Cluster Sims. *Anal. Chem.* **2005**, *77*, 142−149.

(2) Gillen, G.; Simons, D. S.; Williams, P. Molecular Ion Imaging and Dynamic Secondary Ion Mass Spectrometry of Organic Compounds. *Anal. Chem.* **1990**, *62*, 2122−2130.

(3) Sheraz, S.; Barber, A.; Berrueta Razo, I.; Fletcher, J. S.; Lockyer, N. P.; Vickerman, J. C. Prospect of Increasing Secondary Ion Yields in Tof-Sims Using Water Cluster Primary Ion Beams. *Surf. Interface Anal.* **2014**, *46*, 51−53.

(4) Sheraz née Rabbani, S.; Razo, I. B.; Kohn, T.; Lockyer, N. P.; Vickerman, J. C. Enhancing Ion Yields in Time-of-Flight-Secondary Ion Mass Spectrometry: A Comparative Study of Argon and Water Cluster Primary Beams. *Anal. Chem.* **2015**, *87*, 2367−2374.

(5) Wucher, A.; Tian, H.; Winograd, N. A Mixed Cluster Ion Beam to Enhance the Ionization Efficiency in Molecular Secondary Ion Mass Spectrometry. *Rapid Commun. Mass Spectrom.* **2014**, *28*, 396−400.

(6) Tian, H.; Wucher, A.; Winograd, N. Reducing the Matrix Effect in Organic Cluster Sims Using Dynamic Reactive Ionization. *J. Am. Soc. Mass Spectrom.* **2016**, *27*, 2014−2024.

(7) Wucher, A.; Heinrich, R.; Staudt, C., A Method for Quantitative Determination of Secondary Ion Formation Probabilities, In *Secondary Ion Mass Spectrometry (SIMS XII)*, Benninghoven, A., Bertrand, P., Migeon, H. N., Werner, H. W., Eds.; Elsevier Science: 1999; pp 143−146.

(8) Wucher, A., Laser Postionization - Fundamentals. In *Tof-Sims: Materials Analysis by Mass Spectrometry*, 2nd ed.; Vickerman, J. C., Briggs, D., Eds.; IM Publications and SurfaceSpectra: 2013; pp 217−246.

(9) *Crc Handbook of Chemistry and Physics*, 60th ed.; CRC Press: Boca Raton, 1980.
(10) Wucher, A.; Berthold, W.; Oechsner, H., The Charge State of Sputtered Metal Clusters, In *Secondary Ion Mass Spectrometry (SIMS IX)*; Benninghoven, A., Nihei, Y., Shimizu, R., Werner, H. W., Eds.; Wiley & Sons: Yokohama, 1993; pp 100−103.
(11) Wahl, M.; Wucher, A. Vuv Photoionization of Sputtered Neutral Silver Clusters. *Nucl. Instrum. Methods Phys. Res., Sect. B* **1994**, *94*, 36−46.
(12) Wucher, A.; Wahl, M., Cluster Emission in Sputtering, In *Secondary Ion Mass Spectrometry (SIMS X)*; Benninghoven, A., Hagenhoff, B., Werner, H. W., Eds.; Wiley & Sons: Chichester, 1995; pp 65−72.
(13) Heinrich, R.; Wucher, A., Formation of Sputtered Semiconductor Clusters, In *Secondary Ion Mass Spectrometry (SIMS XI)*; Gillen, G., Lareau, J., Bennet, J., Stevie, F., Eds.; Wiley & Sons: Orlando, 1997; pp 949−952.
(14) Heinrich, R.; Wucher, A. Yields and Energy Distributions of Sputtered Semiconductor Clusters. *Nucl. Instrum. Methods Phys. Res., Sect. B* **1998**, *140*, 27−38.
(15) Heinrich, R.; Staudt, C.; Wahl, M.; Wucher, A., Ionization Probability of Sputtered Clusters, In *Secondary Ion Mass Spectrometry (SIMS XII)*; Benninghoven, A., Bertrand, P., Migeon, H.-N., Werner, H. W., Eds.; Elsevier Science: Amsterdam, 1999; pp 111−114.
(16) Meyer, S.; Staudt, C.; Wucher, A. Ionization Probability of Atoms and Molecules Sputtered from a Cesium Covered Silver Surface. *Appl. Surf. Sci.* **2003**, *203−204*, 48−51.
(17) Samartsev, A.; Wucher, A. Yields and Ionization Probabilities of Sputtered In_n Particles under Atomic and Polyatomic Au_m^- Ion Bombardment. *Appl. Surf. Sci.* **2006**, *252*, 6474−6477.
(18) Mazarov, P.; Samartsev, A.; Wucher, A. Determination of Energy Dependent Ionization Probabilities of Sputtered Particles. *Appl. Surf. Sci.* **2006**, *252*, 6452−6455.
(19) Samartsev, A. V.; Heuser, C.; Wucher, A. Ionization Probabilities of Sputtered Indium Atoms under Atomic and Polyatomic Au_m^- Ion Bombardment. *Surf. Interface Anal.* **2013**, *45*, 87−89.
(20) Breuer, L.; Meinerzhagen, F.; Bender, M.; Severin, D.; Wucher, A., Time-of-flight Secondary Ion & Neutral Mass Spectrometry Using Swift Heavy Ions. *Nucl. Instrum. Methods Phys. Res. Sect. B* **2015**, *365*, 482−489.
(21) Kucher, A.; Wucher, A.; Winograd, N. Strong Field Ionization of Beta-Estradiol in the Ir: Strategies to Optimize Molecular Postionization in Secondary Neutral Mass Spectrometry. *J. Phys. Chem. C* **2014**, *118*, 25534−25544.
(22) Popczun, N.; Breuer, L.; Wucher, A.; Winograd, N. On the Sims Ionization Probability of Sputtered Organic Molecules. *J. Am. Soc. Mass Spectrom.* **2017**, DOI: 10.1007/s13361-017-1624-0.
(23) Leone, S. R.; Ahmed, M.; Wilson, K. R. Chemical Dynamics, Molecular Energetics, and Kinetics at the Synchrotron. *Phys. Chem. Chem. Phys.* **2010**, *12*, 6564−6578.
(24) Kucher, A.; Jackson, L. M.; Lerach, J. O.; Bloom, A. N.; Popczun, N. J.; Wucher, A.; Winograd, N. Near Infrared (Nir) Strong Field Ionization and Imaging of C-60 Sputtered Molecules: Overcoming Matrix Effects and Improving Sensitivity. *Anal. Chem.* **2014**, *86*, 8613−8620.
(25) Willingham, D.; Kucher, A.; Winograd, N. Strong-Field Ionization of Sputtered Molecules for Biomolecular Imaging. *Chem. Phys. Lett.* **2009**, *468*, 264−269.
(26) Breuer, L.; Kucher, A.; Herder, M.; Wucher, A.; Winograd, N. Formation of Neutral In_nc_m Clusters under C_{60} Ion Bombardment of Indium. *J. Phys. Chem. A* **2014**, *118*, 8542.
(27) Braun, R. M.; Blenkinsopp, P.; Mullock, S. J.; Corlett, C.; Willey, K. F.; Vickerman, J. C.; Winograd, N. Performance Characteristics of a Chemical Imaging Time-of-Flight Mass Spectrometer. *Rapid Commun. Mass Spectrom.* **1998**, *12*, 1246−1252.
(28) Weibel, D.; Wong, S.; Lockyer, N.; Blenkinsopp, P.; Hill, R.; Vickerman, J. C. A C60 Primary Ion Beam System for Time of Flight Secondary Ion Mass Spectrometry: Its Development and Secondary Ion Yield Characteristics. *Anal. Chem.* **2003**, *75*, 1754−1764.
(29) Wucher, A. Laser Postionization: Fundamentals. In *Tof-Sims: Surface Analysis by Mass Spectrometry*; Vickerman, J. C., Ed.; IM Publications: Chicester, 2001; pp 347−374.
(30) Cheng, J.; Wucher, A.; Winograd, N. Molecular Depth Profiling with Cluster Ion Beams. *J. Phys. Chem. B* **2006**, *110*, 8329−8336.
(31) Wucher, A. A Simple Erosion Dynamics Model for Molecular Sputter Depth Profiling. *Surf. Interface Anal.* **2008**, *40*, 1545−1551.
(32) Wucher, A. Molecular Secondary Ion Formation under Cluster Bombardment: A Fundamental Review. *Appl. Surf. Sci.* **2006**, *252*, 6482−6489.
(33) Willingham, D.; Brenes, D. A.; Wucher, A.; Winograd, N. Strong-Field Photoionization of Sputtered Neutral Molecules for Molecular Depth Profiling. *J. Phys. Chem. C* **2010**, *114*, 5391−5399.
(34) Hankin, S. M.; Villeneuve, D. M.; Corkum, P. B.; Rayner, D. M. Nonlinear Ionization of Organic Molecules in High Intensity Laser Fields. *Phys. Rev. Lett.* **2000**, *84*, 5082−5085.

DOI: 10.1021/acs.jpcc.7b01467
J. Phys. Chem. C 2017, 121, 8931−8937